Journal of Physics: Conference Series

PAPER • OPEN ACCESS

Graphene-layer and graphene-nanoribbon FETs as THz detectors

To cite this article: Y E Matyushkin *et al* 2018 *J. Phys.: Conf. Ser.* **1124** 051054

Graphene-layer and graphene-nanoribbon FETs as THz detectors

Y E Matyushkin[1*], I A Gayduchenko[1], M V Moskotin[1], G N Goltsman[1], G E Fedorov[1], M G Rybin[2], E D Obraztsova[2]
[1]Moscow State University of Education, Moscow, 119991, Russia
[2]Prokhorov General Physics Institute, Moscow, 119991, Russia

Abstract. We report on detection of sub-THz radiation (129-430 GHz) using graphene based asymmetric field-effect transistor (FET) structures with different channel geometry: monolayer graphene, graphene nanoribbons. In all devices types we observed the similar trends of response on sub-THz radiation. The response fell with increasing frequency at room temperature, but increased with increasing frequency at 77 K. Our calculations show that the change in the trend of the frequency dependence at 77 K is associated with the appearance of plasma waves in the graphene channel. Unusual properties of p-n junctions in graphene are highlighted using devices of special geometry.

Introduction

In recent decades there has been an active growth of interest in devices capable of working in the terahertz region of the electromagnetic wave spectrum. This is due, on the one hand, to the development of experimental equipment, and, on the other hand, to a wide variety of possible applications for terahertz devices (medicine, security and communication systems, space exploration, etc.) [1]. A separate important area is the development of high-efficiency terahertz detectors. Carbon nanomaterials like graphene and carbon nanotubes, thanks to its unique optoelectronic properties [2,3], are excellent candidates for the role of a sensitive part of such detectors [4-10]. In this paper, we experimentally compare the response of the detectors with asymmetric contacts (one is the Schottky contact and one – the Ohmic contact) based on monolayer graphene (MLG) and graphene nanoribbons (GNR) to sub-THz radiation. Detection of the radiation in such devices takes place through rectification: due to the asymmetry of the current-voltage (I-V) curve mean current under a harmonically changing non-zero voltage. The latter can be attributed to the unusual properties of the Schottky barrier on graphene-vanadium interface. To study these unusual properties of the barrier, we've made devices with asymmetric contacts based on graphene angled-nanoribbons (GANR: graphene nanoribbons which are at an angle to the metal contacts).

Device fabrication and characterization

The graphene, acting as the conducting channel of a field-effect transistor (FET), was put on top of an oxidized silicon wafer. This silicon substrate was a 480 μm thick silicon wafer covered with a 500 nm thick thermally grown SiO_2 layer. The doped silicon (with the room temperature resistivity of 10 Ω·cm) formes a gate electrode transparent for the sub-THz and THz radiation. Graphene was synthesized using home-made cold-wall CVD-reactor [11]. The growth procedure was adjusted to always give single layer graphene. We made two types of detectors with different channel geometry were further defined using e-beam lithography and etching in oxygen plasma (Figure 1(a,b)) [6].

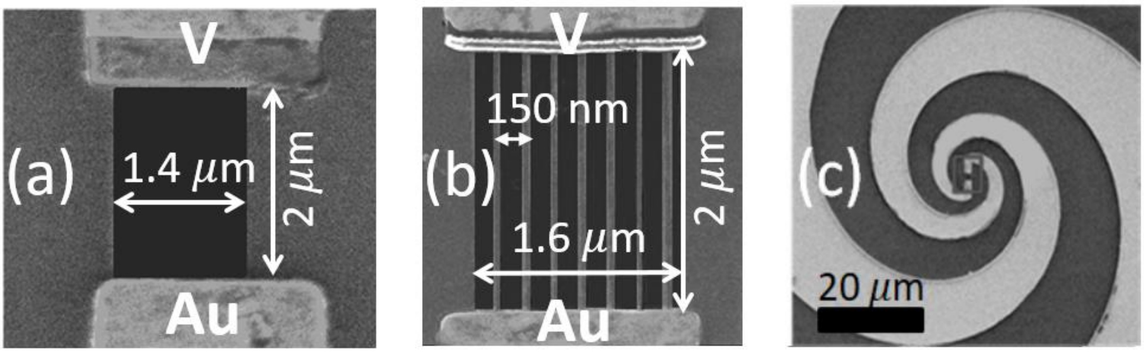

Figure 1(a,b,c). SEM-images of the devices channels made of: **(a)** Graphene monolayer; **(b)** Graphene nanoribbons; **(c)** Logarithmic spiral antenna SEM-image.

The structures of the first type use graphene channel with a width of 1.4 mcm. In the GNR-FETs, graphene was partitioned to form an array of the parallel ribbons connecting the source and drain perpendicular to the electrodes. Width of the ribbons is about 100 nm. The devices (Figure 1(a,b)) are coupled to the radiation with a logarithmic spiral antenna which also serves for DC contacts (Figure 2). The channel of GANR devices is formed by array with the parallel GNRs connecting the source and drain at 45^0 to the electrodes. The source and drain electrodes are made of metals with different work function: vanadium and gold.

The source and drain contacts are connected to a spiral antenna (see Figure 1(a,b)) to ensure a sufficiently broad band device response. We have chosen the log-spiral antenna defined in polar coordinates as $R = R_0 \cdot e^{\varphi/\beta}$ with following parameters: the inner radius of the spiral R_0 equals 5.5 μm, outer radius $R_{max} = 68$ μm the parameter determining the rate of spiral $\beta = 3.2$. Further details of the antenna parameters and its characteristics are presented in Ref. [12]. Importantly we have extensive experience in the manufacture and operation of such antennas (Figure 1(c)).

Experimental setup and results

The fabricated device chip was fixed on flat surface of silicon lens for better radiation coupling (Figure 2). Then lens with chip was put inside optical cryostat. The THz radiation was generated by two backward wave oscillators (BWO) in the frequency range 129-450 GHz. The total losses in the silicon lens and the cryostat optical window do not exceed 5–6 dB.

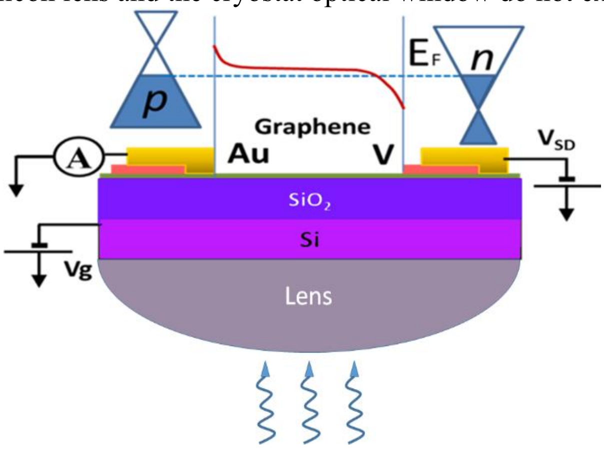

Figure 2. Experimental setup.

As the device is exposed to the radiation the IV curves shifts so that non-zero voltage corresponds to zero current. Figure 3 illustrates the response of the devices to sub-THz radiation at frequency 129 GHz. Comparing the absolute values of the non-zero voltage at zero current for MLG and GNR, it is clearly seen that for GNR this effect is much weaker.

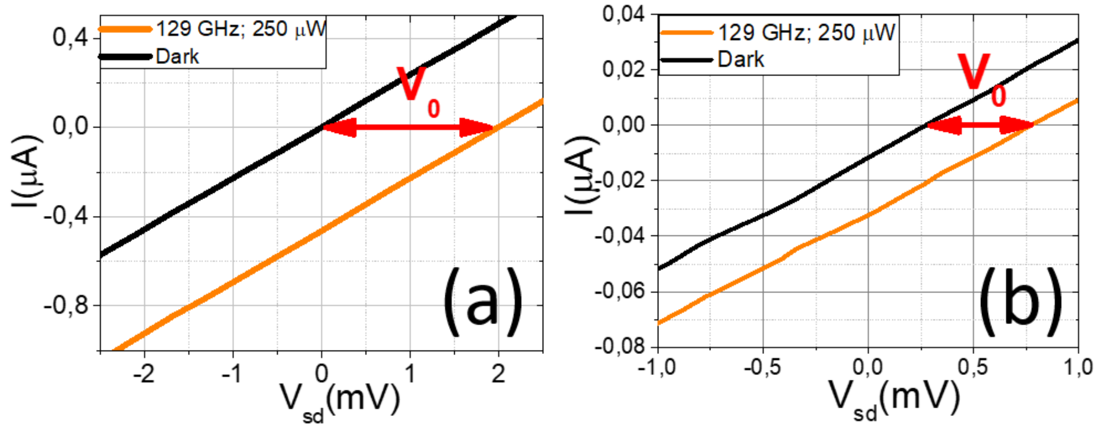

Figure 3(a,b). IV curves of the devices measured with and without sub-THz radiation. **(a)** – monolayer graphene: $V_0 = 2\ mV$; **(b)** – graphene nanoribbon: $V_0 = 0.75\ mV$.

The MLG-FET detector exhibit the room-temperature responsivity from R = 14 V/W at f = 129 GHz to R = 3 V/W at f = 450 GHz (Figure 4). The GNR-FET detector exhibits markedly lower responsivity at this frequency range at 300 K.

The most important feature observed in our experiments is the qualitative change of the frequency dependence of the device responsivity upon a decrease of the temperature from 300 K to 77 K (Figure 4(a)). As the temperature is lowered, the character of the dependence of the responsivity on frequency changes from a decreasing to an increasing one.

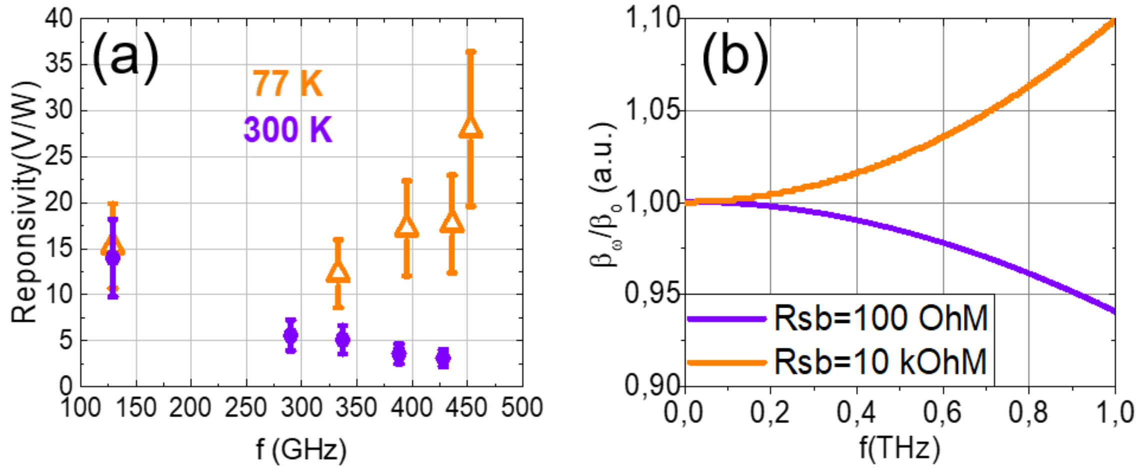

Figure 4(a,b). Responsivity of the graphene monolayer devices as a function of the radiation frequency. **(a)** – experimental results; **(b)** - theoretical calculation with equation (1).

Discussion

In our previous work [6] we have shown that the elastic scattering rate in the CVD-grown graphene used in our experiments does not change in the temperature range between 77K and 300K. We thus can rule out the simple plasmon resonance model of detector response discussed in [13]. Further development of this model accounting for the Schottky barriers capacitance brings to the following formula for the frequency dependence of detector response

$$\frac{\beta_0}{\beta_\omega} = \left| cos\left(\frac{\pi\sqrt{(\omega+i\nu)\omega}}{2\Omega}\right) - ib\frac{(\omega+i\nu)}{\nu}(1-i\omega\tau_s)\right|^{-2} \tag{1}$$

In Eq. (1):

$$\Omega = \frac{\pi^{5/4}v_w}{L}\left[\frac{e^2}{k_g v_W \hbar}W_g\sqrt{n}\right]^{\frac{1}{2}} \tag{2}$$

Ω is the plasma frequency characteristic for the gated channel [14], n is the electron density in the quasi-neutral section of the channel with the length close to the net channel length L, W_g is the gate layer thickness, $v_w \cong 10^8\, cm/s$ is the characteristic electron velocity in graphene, k is the effective dielectric constant (depending on the dielectric constants above and beneath the graphene (or for the graphene nanoribbon*),* $\gamma = \tau^{-1} + \xi(2\pi/\lambda)^2$ [15] is the plasma oscillations decay rate*,* τ^{-1} is the frequency of electron collisions with impurities, phonons, and edges (in graphene), ξ is the electron velocity, $\lambda = 4L$ is the plasma wavelength, β_0 low frequency responsivity*,* $\tau_s = r_s \cdot C_s$ and $\cdot C_s$ are the Schottky junction recharging time (through the Schottky junction) and capacitance, respectively, and $b = L/\sigma_0 r_s = r_{2DES}/r_s$, $r_s = (dJ_s/dV)^{-1}$ is the Schottky junction differential resistance, where $J_s(V)$ is the junction current-voltage characteristics, and r_{2DES} is the dc resistance of the quasi-neutral channel section. The AC conductivity of the 2DES channel is equal to $\sigma_\omega = \sigma_0\tau^{-1}/(\tau^{-1} - i\omega)$, where σ_0 is the DC conductivity.

Based on the temperature evolution of the DC transport, we argue that the only temperature-dependent parameter in the above equations is the Schottky junction recharging time, which is proportional to the barrier resistance. Figure 4(b), show the frequency evolution of the parameter $\beta_0\,/\beta_\omega$ for two values of τ_s. We see that the responsivity is a rising function of frequency for large enough values of τ_s and decreasing otherwise. Other parameters input into the calculations are provided in the figure caption.
In order to explain why a Schottky barrier is formed at the graphene/metal interface we note that the transport of carriers through the p-n junction in graphene depends on the angle between the normal to the junction and the carrier momentum. For normally incident electrons, there is no energy barrier and they shunt the nonlinear transport. At the same time, the current of non-normally incident electrons is a non-linear function of the applied voltage [16,17].
This scenario is confirmed in our case with much smaller signal obtained in the case of the GNR devices. In the case of the nanoribbons, a smaller channel width should lead to a more collimated motion of the charge carriers, so that the fraction of normally incident carriers is larger, causing smaller response value.

To verify these conclusions, we fabricated GANR devices (Figure 5(a)) In order to fabricate these devices we used the same fabrication route as in the case of GNR FETs. The only difference is that the metal edge is not normal to the ribbons. The designed angle is 45 degrees. Such a design ensures that the overall current in the ribbons is directed at an angle of 45 degrees to the p-n junction at the vanadium interface. Following the previous discussion, we argue that in this case larger fraction of carriers encounter an energy barrier at the GANR/V interface and their impact on the device conductance is larger than that in the case of plane graphene. In such case stronger temperature dependence is expected. This prediction is confirmed by the transport measurements reported in the Figure 5(b,c), where conductance of GNR and GANR as a function of gate voltage is shown. We see a

30% drop of conductance in case of GANR as temperature is decreased from 300 to 77 K compared to ~ 15% drop in case of GNR.

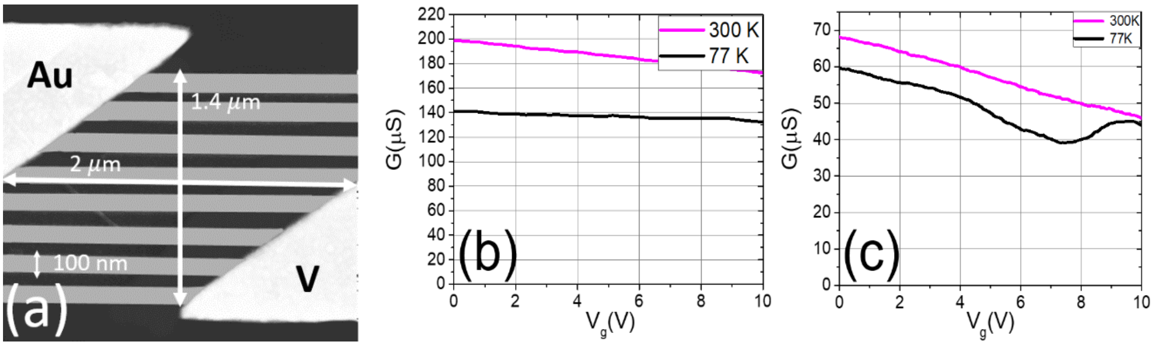

Figure 5(a,b,c). (a) SEM-image of graphene-angled nanoribbons; **(b)** Transfer characteristic of the GANR at 300 K and 77 K; **(c)** Transfer characteristic of the GNR at 300 K and 77 K.

A stronger drop in conductivity at 77K in GANR-devices (30%) than in GNR devices (15%) indirectly suggests the hypothesis that the main detection mechanism is rectification at the Schottky barrier. Investigation of THz radiation detection in GANR asymmetric structures will be subject of our further studies.

Conclusion

Difference between the transport characteristics of the GNR and GANR devices confirms that the properties of the Schottky barrier for the charge carriers in graphene at a p-n junction depends on the angle between the carrier drift velocity and the junction. We have shown that plasma waves can affect the frequency dependence of the response of a graphene lateral Schottky diode even in the graphene devices with rather modest electron mobilities far from the first plasmon resonance, which should be observed at 4.9 THz for our channel geometry and carrier concentration. A strong enhancement of the response is observed at moderately low temperatures when the frequency is increased towards the plasma resonance frequency.

Acknowledgments
This work was supported by the Ministry of Education and Science of Russian Federation (contract №14.583.21.0069, RFMEFI58317X0069). SEM imaging was performed using equipment of MIPT Shared Facilities Center.

References

[1] Masayoshi Tonouchi, 2007 *Nat. Photonics* **1** 97–105
[2] F. Bonaccorso, Z. Sun, T. Hasan, A. C. Ferrari 2010 *Nat. Photonics* **4** 611
[3] A.N. Grigorenko, M. Polini, K.S. Novoselov 2012 *Nat. Photonics* **6** 749
[4] Vicarelli L, Vitiello M S, Coquillat D, Lombardo A, Ferrari A C, Knap W, Polini M, Pellegrini V and Tredicucci A 2012 *Nat. Mat.* **11** 865
[5] Xinghan Cai, Andrei B. Sushkov, Ryan J. Suess, Mohammad M. Jadidi, Gregory S. Jenkins, Luke O. Nyakiti, Rachael L. Myers-Ward, Shanshan Li, Jun Yan, D. Kurt Gaskill, Thomas E. Murphy, H. Dennis Drew & Michael S. Fuhrer 2014 *Nature Nanotechnology* **9** 814
[6] I A Gayduchenko *et al* 2018 *Nanotechnology* **29** 245204
[7] D. A. Bandurin, I. Gayduchenko, Y. Cao, M. Moskotin, A. Principi, I. V. Grigorieva, G. Goltsman, G. Fedorov, and D. Svintsov 2018 *Appl. Phys. Lett.* **112** 141101

IOP Conf. Series: Journal of Physics: Conf. Series **1124** (2018) 051054 doi:10.1088/1742-6596/1124/5/051054

[8] Gayduchenko I, Kardakova A, Fedorov G, Voronov B, Finkel M, Jimenez D, Morozov S, Presniakov M, Goltsman G 2015 *J. Appl. Phys*. **118** 194303
[9] Fedorov G, Gayduchenko I, Titova N, Gazaliev A, Moskotin M, Kaurova N, Voronov B and Goltsman G 2018 *Phys. Status Solidi B* **255** 1700227
[10] Xiaowei He *et all* 2014 *Nano Lett*. **14** (7) 3953–3958
[11] M. Rybin, A. Pereyaslavtsev, T. Vasilieva, V. Myasnikov, I. Sokolov, A. Pavlova, E.A. Obraztsova, A. Khomich, V. Ralchenko, E.D. Obraztsova 2016 *Carbon* **96** 196
[12] Alexander Shurakov, Sergey Seliverstov, Natalia Kaurova, Matvey Finkel, Boris Voronov, and Gregory Goltsman 2012 *Ieee transactions on terahertz science and technology* **2(**4) 400-405
[13] Ryzhii V and Shur M S 2006 *Jpn. J. Appl. Phys*. **45** 42-45
[14] Tomadin A Polini M 2013 *Phys. Rev*. B **88** 205426
[15] Dyakonov M and Shur M 1993 *Phys. Rev. Lett.* **71** 2465
[16] M.I. Katsnelson, K.S. Novoselov, A.K. Geim 2006 *Nature Physics* **2** 620
[17] Sutar S, Comfort E S, Liu J, Taniguchi T, Watanabe K, and Lee J U 2012 *Nano Lett*. **12** 4460−4464